Carbohydrate Research 361 (2012) 141–147

Contents lists available at SciVerse ScienceDirect

Carbohydrate Research

journal homepage: www.elsevier.com/locate/carres

Structural analysis of immunostimulating sulfated polysaccharides from *Ulva pertusa*

Mehdi Tabarsa [a], Sung-Joon Lee [b,*], SangGuan You [a,*]

[a] Department of Marine Food Science and Technology, Gangneung-Wonju National University, 120 Gangneung Daehangno, Gangneung, Gangwon 210-702, South Korea
[b] Division of Food Bioscience and Technology, College of Life Sciences and Biotechnology, Korea University, Seoul 136-713, South Korea

ARTICLE INFO

Article history:
Received 29 June 2012
Received in revised form 5 September 2012
Accepted 5 September 2012
Available online 14 September 2012

Keywords:
Glycosidic linkages
Sulfated polysaccharide
Ulva pertusa
GC–MS
2D-NMR

ABSTRACT

Sulfated polysaccharides were extracted from *Ulva pertusa* and fractionated to obtain the most immunostimulating fraction (F_2). The glycosidic linkages of the polysaccharides in the fraction F_2 were determined using GC–MS and 2D-NMR spectroscopy after chemical modifications, including reduction and desulfation under various conditions. Methanol was used as a sulfate acceptor for the removal of sulfates from the polysaccharides. When the desulfation was carried out at 120 °C, the sulfates were removed up to 90.1% from the F_2 fraction without considerable backbone degradation. The GC–MS analysis as well as NMR spectra revealed that the backbone of the polysaccharides was mainly composed of α-(1→4)-L-rhamnopyranosyl, β-(1→4)-D-glucuronosyl, β-(1→2)-L-rhamnopyranosyl and β-(1→4)-D-xylopyranosyl residues with branches at O-2 position of rhamnose. The sulfate groups were mostly found on glucuronic acid at O-3 position.

1. Introduction

Marine organisms have recently garnered attention as possible sources of bioactive compounds that may be useful as new medicines or food ingredients. Approximately 8000 species of marine algae have been identified and grouped into different classes, including brown algae (Phaeophyta), red algae (Rhodophyta) and green algae (Chlorophyta). Naturally occurring sulfated polysaccharides are commonly found in three major groups of marine algae. However, studies on the sulfated polysaccharides from marine algae have mainly focused on fucoidans, sargassans and glucuronoxylofucans, which are found in brown algae, as well as on carrageenans and agars found in red algae. These sulfated polysaccharides are of particular interest because of their effective bioactivities, such as anticoagulant, antiviral, antitumor, anti-inflammatory, and immunomodulatory activities.[1–6] Sulfated polysaccharides are found in green algae as well, referred to as ulvans, and they also exhibit various biological and pharmacological activities. Recently, it was reported that the sulfated polysaccharides from *Ulva pertusa* were potent antihyperlipidemia agents, which significantly lower the levels of total plasma cholesterol, low-density lipoprotein cholesterol and triglyceride but increase the levels of high-density lipoprotein cholesterol in serum.[7] In addition, ulvan from *Ulva lactuca* was shown to inhibit cancer cell growth by inducing a low cell reactivity to Ulex europaeus-1 lectins.[8] In vivo anticancer activity was also observed by ulvan from *Enteromorpha intestinalis*, which stimulated the immune cells, such as splenocytes and macrophages, inducing nitric oxide or cytokine releases.[9] Ulvan also exhibited antiviral activity against influenza virus by suppressing viral reproduction.[10] Moreover, ulvan was effective against alcohol-induced peptic ulcers.[11]

In a recent study, we isolated sulfated polysaccharides from *U. pertusa* and separated the polysaccharides into three fractions (F_1, F_2 and F_3) using an ion-exchange chromatography.[12] Out of these fractions, fraction F_2 was the most potent stimulator of RAW264.7 macrophages, inducing formation of considerable concentrations of nitric oxide and various cytokines. The biological activity of these polysaccharides has been correlated to their structural properties, which include the composition of the monosaccharide building blocks, their glycosidic linkages, molecular weights as well as the number and chemical nature of the polysaccharides' functional groups.[8,13] The presence of sulfate esters on the backbone of these polysaccharides causes structural elucidation of the glycosidic linkages as well as accurate determination of the position of the sulfate esters themselves to be quite challenging. Thus, accurate structural elucidation requires the application of a desulfation method that can remove the sulfate groups without modifying the backbone of the polysaccharide.

Various desulfation methods have been applied for the structural analysis of sulfated polysaccharides. Miller and Blunt reported that the base in an alkaline-catalyzed desulfation treatment method using tetraethylammonium hydroxide hindered the effective removal of the sulfates in the triethylammonium salt of

* Corresponding authors. Tel.: +82 2 3290 3494; fax: +82 2 2286 1135 (S.-J.L.); tel.: +82 33 640 2853; fax: +82 33 640 2340 (S.G.Y.).
E-mail addresses: junelee@korea.ac.kr (S.-J. Lee), umyousg@gwnu.ac.kr (S.G. You).

0008-6215/$ - see front matter © 2012 Elsevier Ltd. All rights reserved.
http://dx.doi.org/10.1016/j.carres.2012.09.006

ι-carrageenan.[14] Therefore, the acid-catalyzed desulfation treatment method has been preferentially applied for the desulfation of these polysaccharides despite its potential to cause depolymerization of the polysaccharide backbone. Pyridine was added to prevent the polymeric degradation of the polysaccharides during the desulfation process.[14–16] Pyromellitic acid, As_2O_3, NaF and methanol were also added alongside chlorotrimethylsilane as a sulfate acceptor to prevent reversible sulfation.[14,15]

In the present study, the sulfated polysaccharides in fraction F_2, the *U. pertusa* fraction harboring the highest activity for immunomodulation, were structurally characterized using GC–MS and 2D-NMR spectroscopy after they were chemically modified by removal of the sulfate group. Removal of the sulfate allowed accurate structural characterization of the glycosidic linkages found in the polysaccharides of this fraction.

2. Results and discussion

2.1. Desulfation procedure

In an earlier study, the crude sulfated polysaccharide was extracted from *U. pertusa* and fractionated using an ion-exchange chromatograph, which yielded three fractions (F_1, F_2 and F_3) separated based on ionic strengths.[12] Of the three fractions, fraction F_2 was found to be the most potent stimulator of RAW264.7 cells. To accurately elucidate the molecular structure of the sulfated polysaccharide, especially the glycosidic linkages, the polysaccharide needs to be desulfated and reduced without considerable degradation to the backbone of the polymer. Methanol was often used as a sulfate acceptor during the desulfation of sulfated polysaccharides.[16,17] It was shown in Table 1 that considerable desulfation (45.1%) was observed upon adding methanol to the reaction mixture and heating at 80 °C for 60 min. Increasing the reaction time to 120 min increased the removal of sulfate to 58.1%. Further increasing the reaction time to 240 min increased the level of desulfation (up to 68.0%). The polysaccharide yield after desulfation for 60, 120 and 240 min was 59.2%, 60.6% and 57.7%, respectively, showing that methanol allows relatively good sample recovery during the desulfation. Although considerable desulfation up to 70% occurred using methanol at 80 °C, through notably at different reaction lengths, the remaining sulfates on the polysaccharides could prevent accurate determination of the glycosidic linkages. Therefore, higher efficiency of sulfate removal from fraction F_2 polysaccharides may be required for more accurate structural elucidation. Nagasawa et al. reported that reaction temperature was also an important factor in breaking sulfates from the polysaccharide backbone.[18] Therefore, it is unsurprising that additional sulfate removal was observed when a higher reaction temperature (120 °C) was applied to the methanol desulfation treatment (data shown in Table 1). Increasing the temperature to 120 °C significantly raised the desulfation ratio up to 90.1% after a shorter reaction time (40 min). Notably, the HPSEC chromatogram of the desulfated fraction F_2 polysaccharides (DSF_2-6) exhibited a molecular weight distribution similar to that of native F_2 polysaccharides (Fig. 1), indicating that no considerable polymeric degradation occurred during the desulfation process. FT-IR spectra displayed consistent decreases in intensities of peaks at 1247 cm^{-1} and 854 cm^{-1} (Fig. 2), further confirming the removal of sulfates from fraction F_2 polysaccharides. The above results, therefore, suggest that the heating at 120 °C may be more appropriate for desulfation of fraction F_2 polysaccharides than the heating at 80 °C, maintaining the integrity of the polymer backbone, a necessary precursor to the accurate determination of the glycosidic linkages of sulfated polysaccharides.

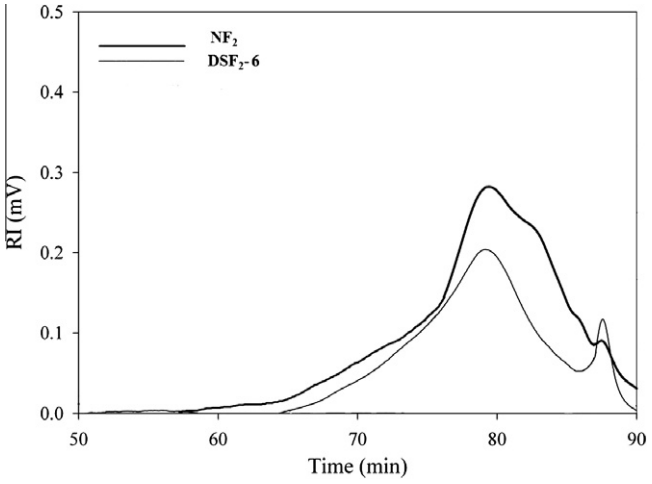

Figure 1. The HPSEC chromatograms of native F_2 polysaccharides (NF_2) and desulfated F_2 polysaccharides by MeOH at 120 °C for 40 min (DSF_2-6).

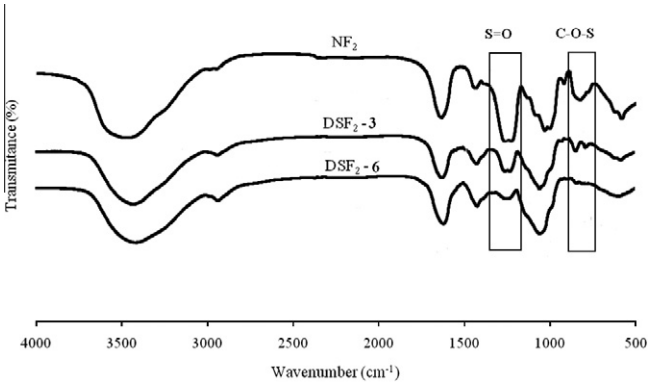

Figure 2. FT-IR spectra of native F_2 polysaccharides (NF_2), desulfated F_2 polysaccharides by MeOH at 80 °C for 240 min (DSF_2-3) and by MeOH at 120 °C for 40 min (DSF_2-6).

2.2. GC–MS analysis

The nature of the glycosidic linkages and sulfate positions of polysaccharides in fraction F_2 were elucidated by methylation

Table 1
Reaction conditions for the desulfation of F_2 polysaccharides

Products	Sulfate acceptor	Temperature (°C)	Time (min)	Sulfate content (%)	Desulfation ratio (%)	Yield (%)
DSF_2-1	MeOH	80	60	15.4 ± 0.2	45.1	59.2
DSF_2-2			120	11.70 ± 0.2	58.1	60.6
DSF_2-3			240	9.90 ± 0.3	68.0	57.7
DSF_2-4		120	10	14.40 ± 0.2	48.4	42.6
DSF_2-5			20	7.66 ± 0.2	72.7	47.0
DSF_2-6			40	2.76 ± 0.2	90.1	46.7

Table 2
Monosaccharide composition (%) of native F_2 polysaccharides (NF_2), reduced F_2 polysaccharides (F_2-RED), and reduced and desulfated F_2 polysaccharides (F_2-RED-DS)

	NF_2 (%)	F_2-RED (%)	F_2-RED-DS (%)
Rhamnose	79.90 ± 0.30	60.90 ± 0.38	58.78 ± 1.10
Xylose	20.00 ± 0.30	8.50 ± 0.74	10.75 ± 1.60
Glucose	—	30.50 ± 0.35	30.40 ± 0.40

analysis of native F_2 polysaccharides, carboxyl-reduced F_2 polysaccharides (F_2-RED) as well as reduced and desulfated F_2 polysaccharides (F_2-RED-DS). For this purpose, respective F_2 samples were methylated by the Ciucanu method.[19] The fully methylated polysaccharides were then subjected to acid hydrolysis, reduction and acetylation. Table 2 shows the monosaccharide profiles of native F_2, F_2-RED and F_2-RED-DS. Native F_2 mainly consisted of rhamnose (79.9%) with considerable amount of xylose (20.0%). When native F_2 was reduced, significant amount of glucose (30.5%) was observed (F_2-RED). This result indicated that the included glucose in native F_2 mostly existed in the acidic form. F_2-RED-DS exhibited similar monosaccharide profiles to that of F_2-RED. The monosaccharide composition of the permethylated F_2 samples was in good agreement with the data of the unmethylated F_2 polysaccharides (Tables 2 and 3). As shown in Table 3, the GC–MS analysis revealed the presence of 2,3-di-*O*-methylxylitol acetates; 2,3,4-tri-*O*-, 3,4-di-*O*-, 2,4-di-*O*-, 2,3-di-*O*- and 3-mono-*O*-methylrhamnitol acetates as well as 2,3,6-tri-*O*- and 2,6-di-*O*-methylglucitol acetates. These results indicated that the sugar residues in fraction F_2 existed as (1→4)-linked xylopyranosyl, (1→2), (1→3) or (1→4)-linked rhamnopyranosyl, (1→4)-linked glucopyranosyl and terminal rhamnopyranosyl residues, which were attached at the branching points of (1→3,4)-linked glucopyranosyl and (1→2,4)-linked rhamnopyranosyl residues.

Comparison of the methylation analysis of native F_2 polysaccharides with that of F_2-RED polysaccharides showed a significant increase in the proportion of 2,6-di-*O*-methylglucitol acetate in F_2-RED without the appearance of new partially methylated alditol acetate (Table 3). The increased proportion of 2,6-di-*O*-methylglucitol acetate after the reduction of native F_2 might be due to the conversion of glucuronic acid into glucose, suggesting that the uronic acid in fraction F_2 likely existed at the (1→3,4)-linked glucopyranosides. The chemical reduction of F_2, on the other hand, resulted in the considerable decreases in the proportions of 2,3,4-tri-*O*-, 2,3-di-*O*-, 3,4-di-*O*-, and 3-*O*-methylrhamnitol acetates. This could potentially be attributed to the significant proportional increase of 2,6-di-*O*-methylglucitol acetate, which appeared to influence the relative ratios of the methylated alditol acetates and thus to decrease the relative proportions of 2,3,4-tri-*O*-, 2,3-di-*O*-, 3,4-di-*O*- and 3-*O*-methylrhamnitol acetates.

Solvolytic desulfation (heating at 120 °C for 40 min in the presence of methanol) resulted in 90% elimination of sulfates from F_2-RED. Methylation analysis showed a significant increase of 2,3,6-tri-*O*-methylglucitol acetate with a concomitant decrease of 2,6-di-*O*-methylglucitol acetate and no considerable changes in the proportions of other methylated alditol acetates (Table 3). This suggested that the sulfate groups were mostly linked at O-3 position of the (1→4)-linked glucopyranosyl residue. Based on the results above, the backbone of the polysaccharide from fraction F_2 was mainly linked by (1→4)-rhamnopyranosyl or (1→4)-glucuronosyl residues with limited occurrence of (1→2)-linked rhamnopyranosyl and (1→4)-linked xylopyranosyl residues. Most branches were connected to the O-3 position of (1→4)-glucopyranosyl or the O-2 of (1→4)-rhamnopyranosyl residues. In addition, the sulfate groups were mostly included in glucose or glucuronic acid at the O-3 position. Similar glycosidic linkages such as (1→4)- and (1→2,4)-linked-rhamnopyranosyl and (1→4)-linked glucuronosyl residues were observed in the sulfated polysaccharides from various types of green seaweeds.[20–24] However, their sulfate groups were located at C-3 of (1→4)-linked rhamnose units and/or C-2 of (1→4)-linked xylose units. The absolute configuration of the sugars was determined by the method of Gerwig et al.,[25] and it was found that rhamnose was present in the L configuration whereas glucuronic acid and xylose were in the D configuration. Compared to these sulfated polysaccharides, the sulfated polysaccharides from *U. pertusa*, especially F_2 fraction, had a unique structural feature in that the sulfate groups were mostly located on the glucose or glucuronic acid at the O-3 position. In a green seaweed, *Monostroma latissimum*, the main backbone of its sulfated polysaccharides consisted of (1→3)-linked α-L-rhamnopyranosyl residues, exhibiting completely different glycosidic linkages from that of the polysaccharide observed in this study.[26] It was, therefore, suggested that significant differences in glycosidic linkages as well as sulfate positions among the sulfated polysaccharides from green seaweeds were mainly derived from the differences in their species.[27,28]

2.3. NMR analyses

The native F_2 polysaccharide and its derivatives (F_2-RED and F_2-RED-DS) were structurally characterized by 1D- and 2D-NMR spectroscopy, including ^1H, ^{13}C, COSY, TOCSY, HMQC, HMBC and NOESY analyses to support the glycosidic linkage analysis, obtained by GC–MS. The ^{13}C NMR spectrum of native F_2 polysaccharide was complex, showing broadened signals consistent with samples containing heterogeneously glycosylated and sulfated rhamnosyl units as well as other monosaccharides such as xylose and glucuronic acids. In addition, the presence of sulfates and branch points in the polysaccharide resulted in spectra with high degrees of overlap (data not shown). Therefore, native F_2 polysaccharide was desulfated and reduced, resulting in polysaccharide derivative F_2-RED-DS. Spectra of F_2-RED-DS were then analyzed to elucidate the glycosidic linkages. However, the disappearance of the downfield signals at 176 ppm from the carboxyl groups of glucuronic acid residues along with the appearance of the signal corresponding to the

Table 3
Glycosidic linkage analysis of native F_2 polysaccharides (NF_2), reduced F_2 polysaccharides (F_2-RED) and reduced and desulfated F_2 polysaccharides (F_2-RED-DS)

Retention time (min)	Methylation	Glycosidic linkage	Peak area (%)		
			NF_2	F_2-RED	F_2-RED-DS
7.9	1,4,5-Tri-*O*-acetyl-2,3-di-*O*-methyl-Xyl	→4)-Xyl-(1→	5.1	4.46	10.7
9.623	1,5-Di-*O*-acetyl-2,3,4-tri-*O*-methyl-Rha	Rha-(1→	25.9	11.5	10.4
11.14	1,2,5-Tri-*O*-acetyl-3,4-di-*O*-methyl-Rha	→2)-Rha-(1→	15.0	6.7	9.0
11.20	1,3,5-Tri-*O*-acetyl-2,4-di-*O*-methyl-Rha	→3)-Rha-(1→	3.8	2.1	1.5
11.38	1,4,5-Tri-*O*-acetyl-2,3-di-*O*-methyl-Rha or 1,4,5-Tri-*O*-acetyl-2,3,6-tri-*O*-methyl-Glu	→4)-Rha-(1→ or →4)-Glu-(1→	30.9	17.1	35.5
11.67	1,3,4,5-Tetra-*O*-acetyl-2,6-Di-*O*-methyl-Glu	→3,4)-Glu-(1→	6.9	30.9	5.0
12.85	1,2,4,5-Tetra-*O*-acetyl-3-mono-*O*-methyl-Rha	→2,4)-Rha-(1→	12.3	6.5	5.6

Table 4
^{1}H and ^{13}C NMR chemical shifts of desulfated F_2 polysaccharides (F_2-DS)

Residue	C-1/H-1	C-2/H-2	C-3/H-3	C-4/H-4	C-5/H-5	C-6/H-6
A →2,4)-α-L-Rha-(1→	94.18/5.27	76.22/3.85	72.10/3.76	76.80/3.66	71.10/3.88	17.16/1.47
B →4)-α-L-Rha-(1→	102.13/5.25	71.30/4.08	70.47/3.95	78.00/3.86	71.80/4.02	17.44/1.48
C α-L-Rha-(1→	93.77/5.01	72.10/4.07	73.10/3.97	71.50/3.82	70.56 /4.15	17.39/1.44
D →2)-α-L-Rha-(1→	93.80/5.00	76.20/4.04	73.20/3.95	71.55/3.80	70.60 /4.11	17.40/1.46
E →4)-β-D-GluA-(1→	103.19/4.88	74.10/3.50	76.00/3.68	79.30/3.84	76.14/4.06	176.00/—
F →4)-β-D-Xyl-(1→	103.17/4.65	73.90/3.49	75.89/3.68	76.02/3.91	67.19/4.16	—

unsubstituted C-6 in the ring protons region (60–65 ppm) caused further overlaps at upfields, resulting in a complex spectrum that precluded the accurate assignment of carbon signals. Therefore, this led us to investigate the glycosidic linkages of F_2 polysaccharides that were only desulfated. This F_2 polysaccharide derivative was labeled F_2-DS. Derivative F_2-DS displayed less complicated ^{1}H and ^{13}C NMR spectra, especially in the non-anomeric regions when compared with the F_2-RED-DS spectra. The ^{1}H NMR spectrum of F_2-DS showed six anomeric proton signals at 5.27, 5.25, 5.01, 5.00, 4.88 and 4.65 ppm in a ratio of nearly 0.25:1.00: 0.37:0.37:0.75:0.35 which were designated as A, B, C, D, E and F, respectively (Table 4, Fig. 3A). The ^{13}C NMR spectrum was also indicative of complex polymers containing two groups of signals in the resonance regions corresponding to anomeric carbons (93.77–103.54 ppm) and ring carbons (70.47–79.30 ppm) as well as three C-CH_3 signals (17.16, 17.39 and 17.44 ppm) and a carboxyl signal at 176.0 ppm (Fig. 3B).

The six ^{1}H resonances from H-1 to H-6 of residue A were assigned from the cross peaks in the COSY and TOCSY spectra (Fig. 4A and B). Based on the proton chemical shifts, the carbon chemical shifts (C-1 to C-6) were assigned from the HMQC spectrum (Fig. 5A). Both proton and carbon chemical shifts indicated that this glycosyl residue was typical of 6-deoxyhexopyranose, suggesting a rhamnosyl moiety. The appearance of an intra-residue correlation between H-1 and H-2 in the NOESY experiment and the J_{H1-C1} coupling constant (~170 Hz) revealed that residue A was α-linked. These results implied that residue A might be α-rhamnose (Table 4). Furthermore, the downfield shift of the C-2 (76.20 ppm) and C-4 (76.80 ppm) carbon signals with respect to the standard values for rhamnose indicated that residue A might be linked by (1→2,4) glycosidic linkages. Therefore, residue A appeared to be α-(1→2,4)-L-rhamnopyranoside. The ^{1}H resonances for H-1 through H-6 of residue B were assigned from the cross peaks in the COSY and TOCSY spectra (Fig. 4A and B). Based on the proton assignments, the chemical shifts of C-1 to C-6 were readily obtained from the HMQC spectrum (Table 4, Fig. 5A). The proton and carbon chemical shifts as well as a small coupling constant value of $J_{H-3,H-4}$ (<3 Hz) for this glycosyl residue implied that

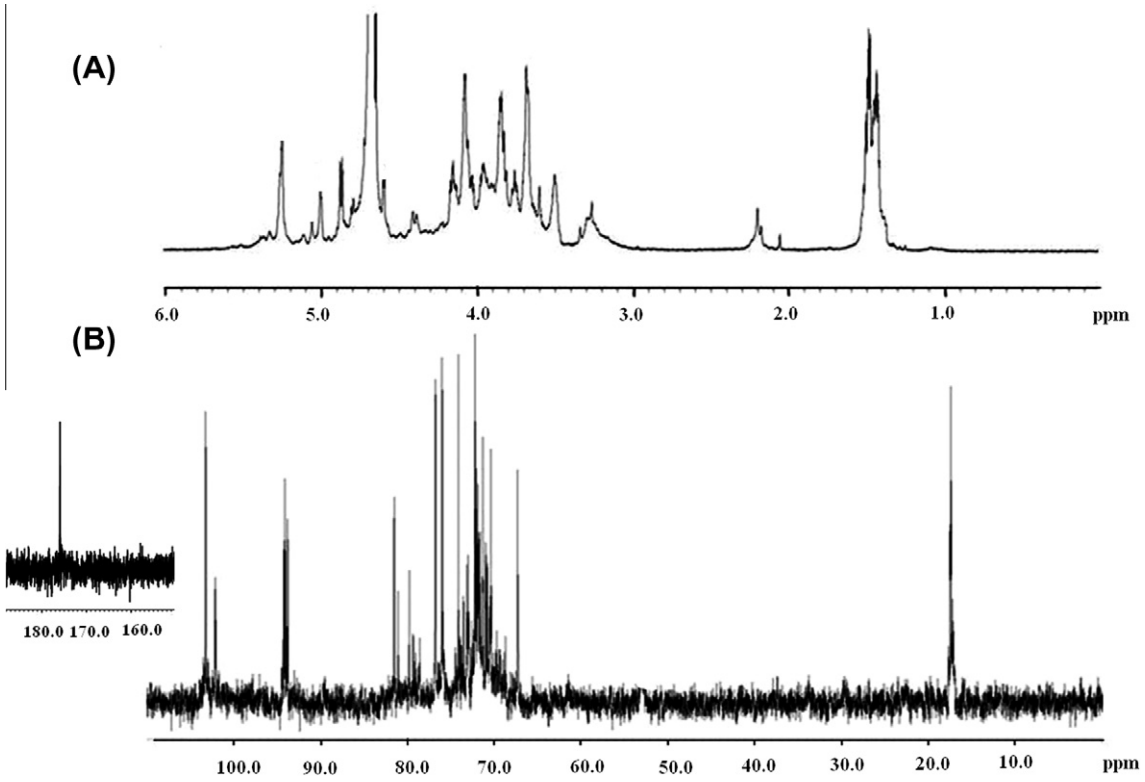

Figure 3. ^{1}H NMR spectrum of desulfated F_2 polysaccharides (F_2-DS) recorded at 600 MHz in D_2O at 50 °C (A) and ^{13}C NMR spectrum of desulfated F_2 polysaccharides (F_2-DS) recorded at 150 MHz in D_2O at 50 °C (B).

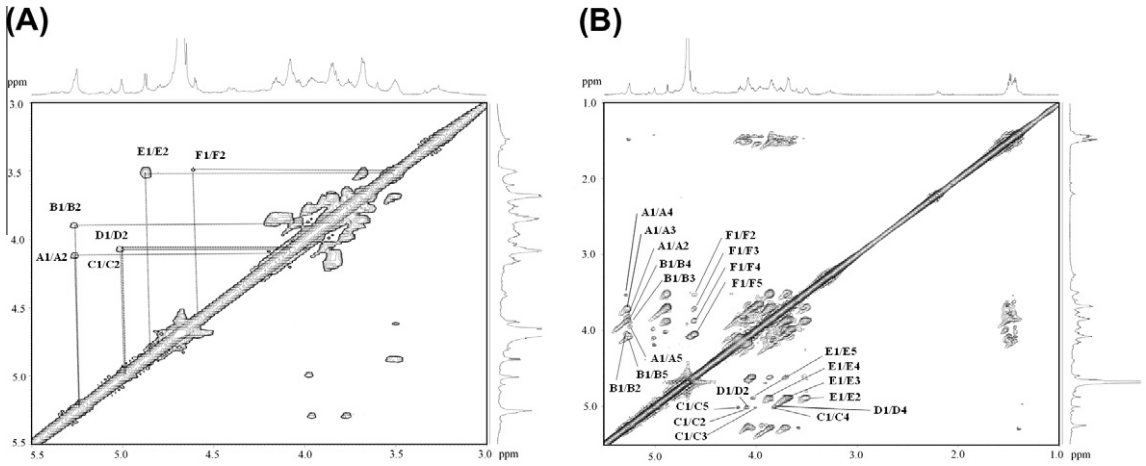

Figure 4. ^{1}H–^{1}H COSY (A) and ^{1}H–^{1}H TOCSY (B) spectra of desulfated F_2 polysaccharides (F_2-DS) recorded in D_2O at 50 °C. A1/2 corresponds to the crosspeak of A H-1 and A H-2, etc.

it might be a rhamnosyl moiety.[29] The downfield shift of the C-4 (78.00 ppm) carbon signal with respect to the standard values for rhamnose indicated that residue B might be connected through (1→4) glycosidic linkages. In addition, a NOESY experiment revealed the intra-residue correlation between H-1 and H-2 (Table 5), implying that residue B was linked at α-anomeric configuration, which was further confirmed by the J_{H1-C1} coupling constant (~170 Hz) from the HMBC spectrum. Therefore, these data suggested that residue B was α-(1→4)-L-rhamnopyranoside. The proton chemical shifts of residue C were assigned for H-1 to H-6 by the COSY spectrum and confirmed by the TOCSY spectrum (Fig. 4A and B). The carbon chemical shifts from C-1 to C-6 were assigned from the HMQC spectrum. The carbon and proton chemical shifts of residue C showed the peculiarities of the rhamnose residue.[30] The shifts of anomeric signals at 5.01 ppm for ^{1}H and 93.77 ppm for ^{13}C with the J_{H1-C1} coupling constant of ~169 Hz suggested that the rhamnose was α-linked. The chemical shifts of residue C with respect to standard values indicated that the moiety C was a nonreducing end α-L-Rha-(1→ residue.[31] The proton and carbon chemical shifts of residue D were assigned from the COSY and HMQC spectra (Figs. 4A and 5A), implying that the moiety D is a rhamnosyl residue. The anomeric signals at 5.00 ppm for ^{1}H and 93.80 ppm for ^{13}C with the J_{H1-C1} coupling constant of ~169 Hz indicated that rhamnose was α-linked. Besides, the downfield shift of the C-2 (76.20 ppm) carbon signal with respect to the standard values for rhamnose indicated that residue D was α-(1→2)-L-rhamnopyranoside. All the ^{1}H resonances for residue E were readily assigned from the COSY spectrum and confirmed from the TOCSY spectrum (Fig. 4A and B). The proton and carbon chemical shifts as well as large coupling constant values of $J_{H-1,H-2}$ (~9.8 Hz) and $J_{H-3,H-4}$ (~10 Hz) for the glycosyl residue implied that it was a glucosyl moiety.[32] The appearance of H-1 as a doublet ($J_{H-1,H-2}$ 8 Hz) in the ^{1}H NMR spectrum and the J_{H1-C1} coupling constant of ~162 Hz suggested that moiety E was β-linked.[30] The relatively downfield carbon chemical shift at 79.30 ppm, caused by the glycosylation effect, was assigned to substitutuent C-4 of residue E.[33] Thus, residue E was identified as β-(1→4)-D-glucopyranuronic acid. The proton chemical shifts of residue F were assigned from the COSY and TOCSY spectra for H-1 to H-5 (Fig. 4A and B). Regarding the very downfield anomeric proton at 4.65 ppm with upfield ^{13}C at 103.17 ppm, moiety F appeared to be a xylopyranose in β-anomeric configuration.[30] The carbon signals from C-1 to C-5 were identified from the HMQC spectrum, among which C-4 was deshielded downfield to a chemical shift of 76.02 ppm. Based on the data obtained, residue F was assigned as β-(1→4)-D-xylopyranoside. The sequence of glycosyl residues was inferred from the HMBC spectrum. The HMBC spectrum revealed the inter-residue correlations between H-1 of residue C and C-2 of residue D, H-1 of residue D and C-2 of residue A, H-1 of residue E and C-4 of residue B, H-4 of residue F and C-1 of

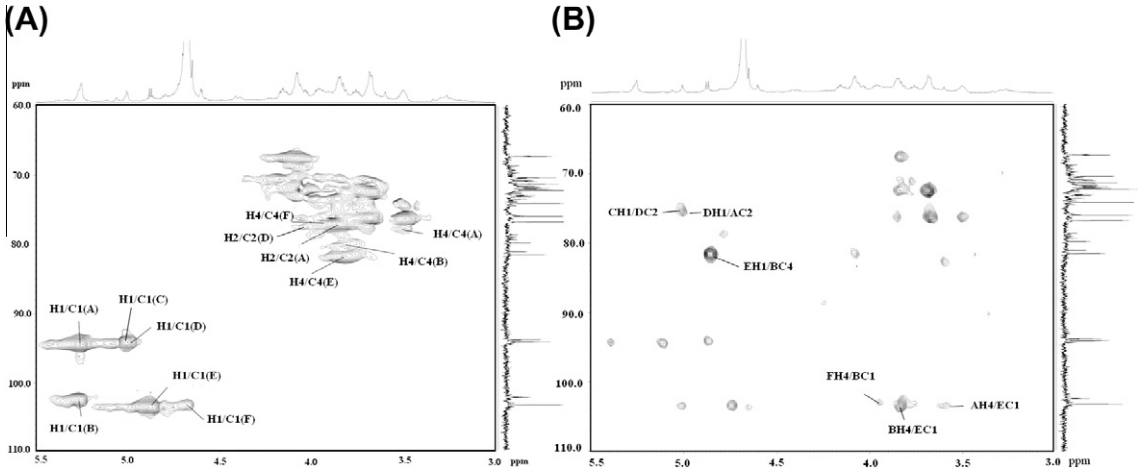

Figure 5. ^{1}H–^{13}C HMQC (A) and ^{1}H–^{13}C HMBC (B) spectra of desulfated F_2 polysaccharides (F_2-DS) recorded in D_2O at 50 °C. H1/C1 (A) corresponds to the crosspeak of A H-1 and A C-1, etc. AH4/DC1 represents the crosspeak of A H-4 and D C-1 that corresponds to glycosidic linkage.

Table 5
NOESY data representing ^1H–^1H connectivities of desulfated F_2 polysaccharides (F_2-DS)

Glycosyl residues	Anomeric proton δ (ppm)	NOE contact protons	
		δ (ppm)	Residue-atom
(A) →2,4)-α-L-Rha-(1→	5.25	3.66	AH4
		3.76	AH3
		3.84	EH4
		3.85	AH2
(B) →4)-α-L-Rha-(1→	5.27	3.84	EH4
		3.91	FH4
		3.95	BH3
		4.08	BH2
(C) α-L-Rha-(1→	5.01	3.97	CH3
		4.04	DH2
		4.15	CH5
(D) →2)-α-L-Rha-(1→	5.00	3.85	AH2
		3.95	DH3
		4.04	DH2
(E) →4)-β-D-GluA-(1→	4.88	3.50	EH2
		3.66	AH4
		3.66	EH3
		3.86	BH4
		4.06	EH5
(F) →4)-ß-D-Xyl-(1→	4.68	3.49	FH2
		3.68	FH3
		3.86	BH4
		3.91	FH5

residue B, H-4 of residue B and C-1 of residue E as well as H-4 of residue A and C-1 of residue E (Fig. 5B). The NOESY data revealed the inter-residue correlations between H-1 of residue A and H-4 of residue E, H-1 of residue B and H-4 of residue E, H-1 of residue B and H-4 of residue F, H-1 of residue C and H-2 of residue D, H-1 of residue D and H-2 of residue A, H-1 of residue E and H-4 of residue A, H-1 of residue E and H-4 of residue B as well as H-1 of residue F and H-4 of residue B (Table 5). Therefore, the data above suggested the F_2 polysaccharide sequence as shown in the following diagram, which showed a good agreement with the GC–MS results.

3. Conclusion

The glycosidic linkage pattern of the immunostimulating sulfated polysaccharide of fraction F_2 from *U. pertusa* was investigated after reduction and desulfation using GC–MS and 2D-NMR spectroscopy. Heating the reaction at 120 °C for 40 min with methanol as a sulfate acceptor was revealed to be the optimal method for desulfating the polysaccharides of fraction F_2. These conditions removed the sulfate group up to 90.1% of the polysaccharides from the fraction F_2 without considerable backbone damage. Reduction and desulfation of the polysaccharides in fraction F_2 was necessary for an accurate determination of the glycosidic linkages via GC–MS analysis. However, only desulfated F_2 polysaccharides that were not reduced yielded interpretable NMR spectra. The GC–MS analysis along with the 1D- and 2D-NMR spectra revealed that the backbone of the F_2 polysaccharide was mainly linked by α-(1→4)-L-rhamnopyranosyl or β-(1→4)-D-glucuronosyl residues in which α-(1→4)-L-rhamnopyranosyl residues are occasionally either branched at the O-2 position or linked to β-(1→4)-D-xylopyranosyl residues. In addition, the sulfate groups were mostly included in glucose or glucuronic acid at the O-3 position.

4. Experimental

4.1. Materials

The extraction and purification of sulfated polysaccharides from *U. pertusa* were carried out using methods described previously.[12] Briefly, to obtain the sulfated polysaccharides, the dried and milled sample of *U. pertusa* was depigmented in 85% ethanol at room temperature overnight. The depigmented sample was extracted into distilled water at 65 °C for 2 h. The crude polysaccharide was then recovered by the addition of ethanol and then subjected to filtration. The crude polysaccharide was fractionated using an ion exchange chromatograph equipped with a DEAE Sepharose fast flow column (17-0709-01, GE Healthcare Bio-Science AB, Uppsala, Sweden). The chromatography yielded three fractions (F_1, F_2 and F_3). The most immunostimulating fraction (F_2) was chosen for further analyses to elucidate the structure of the fraction's component polysaccharides.

4.2. Determination of monosaccharide composition

The composition of the monosaccharides composing the polysaccharide chain was quantitatively determined using an HPLC system that consisted of a pump (Waters 510, Waters, Milford, MA, USA), an injection valve (Model 7010, Rheodyne, Rohnert Park, CA, USA) with a 20 L sample loop, a column (carbohydrate analysis column, 4.6 × 250 mm, Waters, Milford, MA, USA) and an RI detector (Waters 2414). The polysaccharide (6 mg) was dissolved in 2 M trifluoroacetic acid (TFA, 0.3 mL) and hydrolyzed at 120 °C for 90 min. A mixture of acetonitrile and water (80:20, v/v) was used as the mobile phase at a flow rate of 2 mL/min. The absolute configuration of the monosaccharides wase determined by GLC of the acetylated *R*-(-2)-octyl glycosides as described by Gerwig et al.[25]

4.3. Preparation of desulfated polysaccharides

One hundred milligrams of the sulfated polysaccharide from fraction F_2 was dissolved in distilled water (10 mL), eluted with pyridine from a Dowex 50 W resin column (X-8, H^+,1 × 15 cm), then lyophilized to yield the polysaccharide-pyridinium salts. The desulfation from the polysaccharide-pyridinium salts (100 mg) was carried out under various conditions using MeOH as a sulfate acceptor, temperatures (either 80 or 120 °C) and reaction times (ranging from 10 to 240 min). After desulfation, the reaction mixture was dialyzed in a membrane (#3247027, Spectrum Laboratories, Compton, CA, USA) against distilled water for three successive days then lyophilized to obtain the desulfated samples. The sulfate content of the polysaccharides was determined by the $BaCl_2$–gelatin method using K_2SO_4 as a standard.[33]

4.4. Carboxyl-reduction of desulfated polysaccharides

The reduction of the uronic acids was conducted by a slightly modified method to the one reported by Taylor and Conrad.[34] Briefly, the acidic polysaccharide (100 mg) was dissolved in distilled water (10 mL) and reacted in the presence of 200 mg of 1-ethyl-3-(3-dimethylaminopropyl)-carbodiimide (EDC) at pH 4.7 for 90 min at room temperature. Next, 2.0 M sodium borodeuteride (10 mL) was added drop wise and allowed to react further for 90 min at pH 7.0. The reduced polysaccharide was obtained by the dialysis of the reaction mixtures against distilled water using a membrane (#3247027, Spectrum Laboratories) and then lyophilization.

4.5. High performance size exclusion refractive index profile

Sulfated polysaccharide (4 mg) was dissolved in 2 mL of distilled water and heated in a microwave bomb (#4872, Parr Instrument Co., Moline, IL, USA) for 30 s. The heated sample solution was filtered through a cellulose acetate membrane (3.0 μm pore size, Whatman International) before injection into the high performance size exclusion chromatography column, which was linked to a UV, multi-angle laser light scattering and refractive index

detection (HPSEC-MALLS-RI) system. The HPSEC-MALLS-RI system included a pump (Waters 510, Milford, MA, USA), an injector valve with a 200 μL sample loop (model 7072, Rheodyne), SEC columns (TSK G5000 PW, 7.5 × 600 mm; TosoBiosep, Mongomeryville, PA, USA), a UV detector at 280 nm (Waters 2487), a multi-angle laser light scattering detector (HELEOS, Wyatt Technology Corp, Santa Barbara, CA, USA) and a refractive index detector (Waters 2414). An aqueous solution of 0.15 M $NaNO_3$ and 0.02% NaN_3 was used for the mobile phase at a flow rate of 0.4 mL/min. The M_w and R_g were calculated using the ASTRA 5.3 software (Wyatt Technology Corp.). The MALLS detector was normalized, and the volume delays of the UV, MALLS and RI detectors were calculated using bovine serum albumin (BSA) as a standard.

4.6. Glycosidic linkage analysis

Analysis of the glycosidic linkages in the polysaccharides was carried out using a slightly modified version of the Ciucanu method.[19] The polysaccharide (2–3 mg) was dissolved in 0.5 mL DMSO (dimethylsulfoxide) under nitrogen and then methylated with 0.3 mL CH_3I and NaOH (20 mg). Partially methylated alditol acetates were prepared from fully methylated samples by acid hydrolysis of the methylated samples with 4 M TFA at 100 °C for 6 h. The hydrolysates were then reduced in distilled water with $NaBD_4$ then acetylated with acetic anhydride. These partially methylated alditol acetate derivatives were then analyzed by a gas chromatography-mass spectrometry (GC–MS) system (6890 N/MSD 5973, Agilent Technologies, Santa Clara, CA) containing a HP-5MS capillary column (30 m × 0.25 mm × 0.25 μm) (Agilent Technologies, Santa Clara, CA). Helium was used as the carrier gas and was maintained at a constant flow rate of 1.2 mL/min. The oven conditions included a temperature program as follows: from 160 to 210 °C over 10 min and then to 240 °C over 10 min. Thus, the temperature gradient was 5 °C/min. The inlet temperature was kept constant at 250 °C. The mass range was set to measure between 35 and 450 *m*/*z*. Peak assignments were based on retention times and mass spectra.

4.7. Spectroscopic methods

Fourier-transform infrared (FTIR) spectra of the polysaccharides were recorded on a Tensor 27 spectrometer (Bruker, Germany) that uses a KBr pellet system. For nuclear magnetic resonance spectrometry (NMR) analysis, the lyophilized sample was dissolved in D_2O (30 mg/mL). The NMR spectrum of the dissolved sample solution was recorded at 50 °C using a JEOL ECA-600 spectrometer (JEOL, Akishima, Japan) equipped with a 5 mm multi-nuclear auto-tuning TH tunable probe at a base frequency of 150 MHz for ^{13}C and 600 MHz for ^{1}H. Chemical shifts were expressed in ppm. Acetone was used as an internal standard and displayed shifts at 31.45 and 2.22 ppm for ^{13}C and ^{1}H, respectively. The COSY spectra (^{1}H–^{1}H) were recorded with an F2 time domain of 1280 points and an F1 time domain of 512 points. The TOCSY spectra (^{1}H–^{1}H) were recorded at mixing time of 50 ms and with an F2 time domain of 1280 points and an F1 domain of 512 points. HMQC spectra (^{1}H–^{13}C) were recorded with an F2 time domain of 1024 points and an F1 time domain of 512 points. HMBC spectra (^{1}H–^{13}C) were recorded with an F2 time domain of 1024 points and an F1 time domain of 512 points with a 1.5 s delay for evolution of long-range couplings. NOESY spectra (^{1}H–^{1}H) were recorded with an F2 time domain of 1024 points and an F1 time domain of 512 points with a mixing time of 0.5 s.

References

1. Mao, W. J.; Fang, F.; Li, H. Y.; Qi, X. H.; Sun, H. H.; Chen, Y., et al *Carbohydr. Polym.* **2008**, *74*, 834–839.
2. Cassolato, J. E. F.; Noseda, M. D.; Pujol, C. A.; Pellizzari, F. M.; Damonte, E. B.; Duarte, M. E. R. *Carbohydr. Res.* **2008**, *343*, 3085–3095.
3. You, S. G.; Yang, C.; Lee, H. Y.; Lee, B. Y. *Food Chem.* **2010**, *119*, 554–559.
4. Saito, A.; Yoneda, M.; Yokohama, S.; Okada, M.; Haneda, M.; Nakamura, K. *Hepatology Res.* **2006**, *35*, 190–198.
5. Zhou, G.; Sheng, W.; Yao, W.; Wang, C. *Pharmacol. Res.* **2006**, *53*, 129–134.
6. Karnjanapratum, S.; You, S. G. *Int. J. Biol. Macromol.* **2011**, *48*, 311–318.
7. Pengzhan, Y.; Ning, L.; Xiguang, L.; Gefei, Z.; Quanbin, Z.; Pengcheng, L. *Pharmacol. Res.* **2003**, *48*, 543–549.
8. Kaeffer, B.; Benard, C.; Lahaye, M.; Blottiere, H. M.; Cherbut, C. *Planta Med.* **1999**, *65*, 527–531.
9. Jiao, L.; Li, X.; Li, T.; Jiang, P.; Zhang, L.; Wu, M., et al *Int. Immunopharmacol.* **2009**, *9*, 324–329.
10. Ivanova, V.; Rouseva, R.; Kolarova, M.; Serkedjieva, J.; Rachev, R.; Manolova, N. *Prep. Biochem.* **1994**, *24*, 83–97.
11. Hwang, H. J.; Kwon, M. J.; Kim, I. H.; Nam, T. *J. Food Chem. Toxicol.* **2008**, *46*, 2653–2657.
12. Tabarsa, M.; Han, J. H.; Kim, C. Y.; You, S. G. *J. Med. Food* **2012**, *15*, 135–144.
13. Qi, H.; Zhang, Q.; Zhao, T.; Chen, R.; Zhang, H.; Niu, X., et al *Int. J. Biol. Macromol.* **2005**, *37*, 195–199.
14. Miller, I. J.; Blunt, J. W. *Carbohydr. Res.* **1998**, *309*, 39–43.
15. Kolender, A. A.; Matulewicz, M. C. *Carbohydr. Res.* **2004**, *339*, 1619–1629.
16. Navarro, D. A.; Flores, M. L.; Stortz, C. A. *Carbohydr. Polym.* **2007**, *69*, 742–747.
17. Li, B.; Wei, X. J.; Sun, J. L.; Xu, S. Y. *Carbohydr. Res.* **2006**, *341*, 1135–1146.
18. Chattopadhyay, K.; Mandal, P.; Lerouge, P.; Driouich, A.; Ghosal, P.; Ray, B. *Food Chem.* **2007**, *104*, 928–935.
19. Nagasawa, K.; Inoue, Y.; Kamata, T. *Carbohydr. Res.* **1977**, *58*, 47–55.
20. Ciucanu, I.; Kerek, F. *Carbohydr. Res.* **1984**, *13*, 209–217.
21. Ray, B. *Carbohydr. Polym.* **2006**, *66*, 408–416.
22. Lahaye, M.; Ray, B. *Carbohydr. Res.* **1996**, *283*, 161–173.
23. Lahaye, M.; Brunel, M.; Bonnin, E. *Carbohydr. Res.* **1997**, *304*, 325–333.
24. Lahaye, M.; Inizan, F.; Vigouroux, J. *Carbohydr. Polym.* **1998**, *36*, 239–249.
25. Gerwig, G. J.; Kamerling, J. P.; Vliegenthart, J. F. G. *Carbohydr. Res.* **1978**, *62*, 349–357.
26. Li, H.; Mao, W.; Zhang, X.; Qi, X.; Chen, Y.; Chen, Y., et al *Carbohydr. Polym.* **2011**, *85*, 394–400.
27. Jiao, G.; Yu, G.; Zhang, Z.; Ewart, H. S. *Mar. Drugs* **2011**, *9*, 196–223.
28. Lahaye, M.; Robic, A. *Biomacromolecules* **2007**, *8*, 1765–1774.
29. Mondal, S.; Das, D.; Roy, S. K.; Islam, S. S. *Carbohydr. Res.* **2012**, *354*, 74–78.
30. Lahaye, M. *Carbohydr. Res.* **1998**, *314*, 1–12.
31. Agrawal, P. K. *Phytochemistry* **1992**, *31*, 3307–3330.
32. Mondal, S.; Chakraborty, I.; Rout, D.; Islam, S. S. *Carbohydr. Res.* **2006**, *341*, 878–886.
33. Dubois, M.; Gilles, K. A.; Hamilton, J. K.; Rebers, P. A.; Smith, F. *Anal. Chem.* **1956**, *28*, 350–356.
34. Taylor, R. L.; Conrad, H. E. *Biochemistry* **1972**, *11*, 1383–1388.